Pharmacogn J. 2024; 16(4): 816-830
A Multifaceted Journal in the field of Natural Products and Pharmacognosy
www.phcogj.com

Original Article

In Silico Study of Eugenol, Cinnamaldehyde, Ethyl Para Methoxycinnamate, Curcumin, and Hesperidin as Antibacterials Against Levofloxacine-Resistant Indonesian *H. pylori* Strains

Musa Ghufron[1], Sukardiman[2], Rahadian Zainul[3,4]*, Muhammad Miftahussurur[5], Arif Nur Muhammad Ansori[6,7,8], Mochammad Aqilah Herdiansyah[8,9]

[1]*Doctoral Program of Medicine, Faculty of Medicine, Universitas Airlangga, Surabaya, INDONESIA.*

[2]*Department of Pharmaceutical Sciences, Faculty of Pharmacy, Universitas Airlangga, Surabaya, INDONESIA.*

[3]*Department of Chemistry, Faculty of Mathematics and Natural Sciences, Universitas Negeri Padang, Padang, INDONESIA.*

[4]*Center for Advanced Material Processing, Artificial Intelligence, and Biophysic Informatics (CAMPBIOTICS), Universitas Negeri Padang, Padang, INDONESIA.*

[5]*Department of Internal Medicine, Faculty of Medicine, Universitas Airlangga, Surabaya, INDONESIA.*

[6]*Postgraduate School, Universitas Airlangga, Surabaya, INDONESIA.*

[7]*Uttaranchal Institute of Pharmaceutical Sciences, Uttaranchal University, Dehradun, INDIA.*

[8]*Virtual Research Center for Bioinformatics and Biotechnology, Surabaya, INDONESIA.*

[9]*Department of Biology, Faculty of Science and Technology, Universitas Airlangga, Surabaya, INDONESIA.*

Correspondence

Rahadian Zainul

Department of Chemistry, Faculty of Mathematics and Natural Sciences; Center for Advanced Material Processing, Artificial Intelligence, and Biophysic Informatics (CAMPBIOTICS), Universitas Negeri Padang, Padang, INDONESIA.

E-mail: rahadianzmsiphd@fmipa.unp.ac.id

History

- Submission Date: 16-06-2024;
- Review completed: 26-07-2024;
- Accepted Date: 02-08-2024.

DOI : 10.5530/pj.2024.16.135

Article Available online

http://www.phcogj.com/v16/i4

ABSTRACT

The occurrence of antibacterial resistance has become a global concern. The results of previous studies revealed many cases of antibacterial resistance of levofloxacin in *H. pylori* strains originating from Indonesia. Conventional attempts to obtain new antibacterial agents usually take a long time, other efforts are needed to speed up discovery. Databases that provide the structure of DNA gyrases cannot fully provide what is needed. This study aims to obtain the three-dimensional structure of DNA gyrase of the Indonesian *H. pylori* strain so that it can be used to simulate the interaction process of compounds that have the potential to be anti-*H. pylori* through *in silico* studies. This study used *in silico* methods to predict the absorption, distribution, metabolism, excretion, and toxicology of potential compounds. The next process involves screening for drug similarity based on criteria set by Muegge, Egan, Veber, Lipinski, and Ghose. The three-dimensional structure of DNA gyrase is formed from several samples of amino acid sequences from the Indonesian *gyrA* and *gyrB H. pylori* strains. Eligible potential compounds were subjected to molecular docking studies on *gyrA* and *gyrB* to obtain the best score. The three-dimensional structure of the Indonesian *gyrA* and *gyrB H. pylori* strains has been obtained. Eugenol, cinnamaldehyde, and ethyl p-methoxycinnamate were more easily absorbed compared to curcumin and levofloxacin as controls. Curcumin and hesperidin show poor absorption and longer distribution in the gastric mucosa, thus allowing long-term interaction with *H. pylori*. All compounds do not inhibit cytochrome P450, can be excreted by the body, and are non-toxic. The prediction of drug similarity passes only through curcumin and ethyl p-methoxycinnamate. The results of molecular docking concluded that curcumin and hesperidin had better scores than levofloxacin. Curcumin has the most potential as an anti-*H. pylori*.

Keywords: Bioinformatics, Phytochemical compound, Anti-*H. pylori*, *In silico*, Medicine.

INTRODUCTION

Helicobacter pylori is estimated to infect more than half of the world's population, although levels vary between regions.[1] A higher prevalence of infection is found in developing countries compared to developed countries.[2] The highest prevalence is found in residents in the regions of Latin America, the Caribbean, Nigeria, Serbia, South Africa, Nicaragua, and Colombia. Low prevalence can be found in North America, Belgium, Sweden, Ghana, and Yemen. The prevalence of infection in the European region varies between twenty to forty percent.[3] Other findings revealed the highest prevalence of infection in regions of Africa, South America, and Western Asia, Nigeria, Portugal, Estonia, Kazakhstan, and Pakistan. The lowest prevalence is found in Oceania, Western Europe, North America, Switzerland, Denmark, New Zealand, Australia, and Sweden. The prevalence varies widely in large areas, for example, in rural Western Australia while in other areas it is lower. Alaska Natives are infected more than any other region of the Americas.[4] The incidence of *H. pylori* infection is also found in various parts of Indonesia including Bali, Java, Kalimantan, Papua, Sumatra, and Sulawesi.[5] The spread of infection is found in Papuan, Batak, Bugis, Chinese, Dayak, and Javanese tribes in Indonesian territory.[6]

Long-term *H. pylori* infection will cause the risk of dyspeptic symptoms to gastric cancer.[7] Helicobacter pylori is the first microbiota carcinogen established by the International Agency for Research on Cancer (IARC) of the World Health Organization (WHO). *H. pylori* infection is very likely a cause of severe stomach diseases such as peptic ulcers and stomach cancer. The disease has caused the death of more than one million lives each year.[1] *H. pylori* is clinically associated with gastritis complaints and complications that can long cause stomach cancer.[8] *H. pylori* infection will cause a complex syndrome of atrophic gastritis and in the long term can cause stomach cancer.[9] Although there is also a family history of stomach cancer, *H. pylori* infection also remains one of the main risk factors.[10] Cancer deaths worldwide are due to stomach cancer, while *H. pylori* infection is the strongest risk factor. *H. pylori* is a specific microbiota that resides in the stomach and is specifically associated with the occurrence of stomach cancer.[11]

The development of information technology has been increasingly rapid to get drugs that are easier and faster. Information provider sites have provided a lot of data to use in drug discovery research.[12] New drug discovery uses information technology in the form of computer-aided drug discovery (*in silico*). Computer drug design by utilizing advances in

Cite this article: Ghufron M, Sukardiman, Zainul R, Miftahussurur M, Ansori ANM, Herdiansyah MA. *In Silico* Study of Eugenol, Cinnamaldehyde, Ethyl Para Methoxycinnamate, Curcumin, and Hesperidin as Antibacterials Against Levofloxacine-Resistant Indonesian *H. pylori* Strains. Pharmacogn J. 2024;16(4): 816-830.

information technology can be done to identify and develop chemical compound structures, physicochemical properties, and biological activities.[13] *In silico* approaches have been increasingly taken to identify active scaffolds and guide subsequent optimization processes from target structure prediction, integrating sequence data, binding side assessment, and target validation, to molecular docking assessment functions.[14]

For years, clarithromycin has been used as one of the first-line treatments for *H. pylori* infections. However, current reality indicates that clarithromycin has largely proven to be ineffective due to the increasing incidence of resistance.[15] Resistance to levofloxacin also increases. The emergence of resistance in different regions poses a threat. Various *H. pylori* resistance to levofloxacin has been documented at significant levels in strains from several regions around the world.[16] Resistance to all three antibiotics has been reported in Southeast Asia, South Asia, Nepal, and even Europe.[17-18] High levels of resistance to levofloxacin have also been found in Indonesian strains.[19] Given these conditions, alternative approaches in the treatment of *H. pylori* infections must be promptly developed.

Levofloxacin, a quinolone class of antibacterial, is an inhibitor of the DNA Gyrase protein. As a result of inhibiting DNA gyrase, relaxation of positively supercoiled DNA will be prevented so that the process of separating DNA chromosomes that have been replicated into daughter cells will be disrupted.[20] DNA Gyrase is carried by the *gyrA* and *gyrB* genes.[21] Several point mutations have been found in the *gyrA* and *gyrB* genes in Indonesian strains of *H. pylori*.[19] Levofloxacin resistance is very possible due to the presence of point mutations in this gene.

Advances in information technology have accelerated the discovery of potential therapy compounds. Various databases can support the process of developing antibacterial discoveries, however, they cannot fully provide all the necessary data.[22] The three-dimensional structure of *gyrA* and *gyrB H. pylori* needed to find antibacterial is still very limited.[23] This research was conducted to get a three-dimensional structure of *gyrA* and *gyrB H. pylori* Indonesian strain. The three-dimensional structure will be used in simulating the interaction of potential compounds with *gyrA* and *gyrB H. pylori* by *in silico* study. Molecular docking is a trustworthy way to simulate the interaction of potential compounds with receptor proteins.[14]

Indonesia has a lot of biodiversity but still not much that is used as medicine. There are many opportunities for drug discovery from various Indonesian plants that contain medicinal compounds. Hesperidin (*Citrus aurantifolia*), curcumin *(Curcuma domestica)*, cinnamaldehyde *(Cinnamomum burmannii)*, ethyl para-methoxycinnamate *(Kaempferia galanga)*, and eugenol *(Eugenia caryophyllata)* are known as antimicrobial agents.[24-30] Research on various compounds is generally carried out in vitro but not many have been done *in silico* studies. The description of oral administration of various compounds is needed to see the process of absorption, distribution, metabolism, and excretion (ADME), as well as the risk of toxicity (T) in the body. Screening of selection requirements for similarity with drugs on various compounds should also be carried out.[31] The next process will describe the condition of the compound when interacting with *gyrA* and *gyrB H. pylori.* This compound has great potential as an anti-*H. pylori* but still needs to be proven further regarding its binding to the active sites of *gyrA and gyrB*. This research is important because of the growing number of Indonesian *H. pylori* strains that are resistant to levofloxacin. This study aims to provide evidence of the potential of hesperidin, curcumin, cinnamaldehyde, ethyl para-methoxycinnamate, and eugenol as anti-*H. pylori* agent through *in silico* studies.[32-33]

METHODS

This research is a type of experimental analysis research conducted *in silico*. The research design used was a randomized post-test-only experimental design with control. The study begins with screening through prediction of the process of absorption, distribution, metabolism, excretion, and toxicity (ADMET) of compounds in the body and to obtain compounds that meet the requirements as drugs. Compounds that have been confirmed to meet the requirements are carried out molecular docking on *gyrA* and *gyrB*. The amino acid sequences of *gyrA* and *gyrB* proteins were obtained from *H. pylori* populations from gastric biopsies of several people from various regions in Indonesia.[19] The sample number consisted of ten amino acid sequences *gyrA* and ten *gyrB*.

Instruments

An *in silico* study will be carried out using Core I.7 computer hardware with the Windows 11, 64-bit, 16 GB RAM operating system. The software that will be used directly on the provider's site is the Microsoft Edge browser to search the database provider's site and the software provider, the database provider's information about the structure of the compound Eugenol, Cinnamaldehyde, Ethyl Para-methoxycinnamate, Curcumin, Hesperidin, and Levofloxacin in the PubChem Compound Database (http://pubchem.ncbi.nlm.nih.gov) owned by National Library of Medicine, National Center for Biotechnology Information.[34] Software providers for similar prediction analysis as drugs and the formation of three-dimensional protein structures from Swiss Institute of Bioinformatics.[35-37] Software Provider for Analysis of Biological Activity Prediction Analysis (ADMET) the PKCSM site owned by Collaboration between Instituto Rene Ranchou Fiocruz Minas, The University of Melbourne, and the University of Cambridge (https://biosig.lab.uq.edu.au/pkcsm/prediction).[38,62] The downloaded software and installed on a computer are Mollegro Virtual Docker (MVD) software which is used to find the location of the active site and conduct a virtual molecular tightening test and Discovery Studio Visualizer 4.1 software (http://accelrys.com/resour) which uses to conduct a two-dimensional analysis of residual interactions, namely position, type, number, and distance of interaction between compounds (Eugenol, Cinnamaldehyde, Ethyl Para-methoxycinnamate, Curcumin, Hesperidin, Levofloxacin) and DNA gyrase as a result of the molecular docking that has been carried out.[39-40]

MATERIALS

The compounds hesperidin, curcumin, cinnamaldehyde, ethyl para-methoxycinnamate, eugenol, and Levofloxacin were downloaded from the PubChem database and stored as smiles.[34] The *gyrA* and *gyrB* amino acid sequence of *H. pylori* data used comes from the Laboratory of The Institute of Tropical Disease (ITD) Airlangga University of Surabaya, Indonesia, and Faculty of Medicine Oita University of Yufu, Japan.[5] Chemical structure of Eugenol, Cinnamaldehyde, Ethyl Para-methoxycinnamate, Curcumin, and Hesperidin downloaded from the PubChem Compound Database Provider (http://pubchem.ncbi.nlm.nih.gov).

Determination of Compounds That Meet Drug Similarity Criteria and ADMET Prediction

The data were entered into the online pcKSM software to obtain absorption, distribution, metabolism, excretion, and toxication (ADMET) prediction data of these various compounds.[64] The data was also entered into the online SwissADME software to get a prediction of similarity to a drug.[37-38]

GyrA and *gyrB* Preparation

The Indonesian *gyrA* and *gyrB H. pylori* strain amino acid sequence data was mapped using Bioedit and translated. The translation results are sent to the Swiss-MODEL software provider for three-dimensional structure formation.[36]

Table 1. The table that shows the ADMET prediction results

Compounds	Absorption		Distribution		Metabolism		Excretion	Toxicity		
	Caco2 permeability (log Papp in 10^{-6} cm/s)	Human Intestinal absorption (%)	VDss (log L/kg)	BBB permeability (log BB)	CYP2D6 substrate and inhibition	CYP3A4 substrate and inhibition	Total Clearance (log ml/min/kg)	Max. tolerated dose (log mg/kg/day)	Oral Rat Acute Toxicity (LD50) (mol/kg)	Hepatotoxicity
Eugenol	**1.559**	**92.041**	0.24	**0.374**	No	No	0.282	1.024	2.118	No
Cinnamaldehyde	**1.634**	**95.015**	0.266	**0.436**	No	No	0.203	0.876	1.88	No
Curcumin	-0.093	**82.19**	**-0.215**	-0.562	No	Yes	-0.002	0.081	1.833	No
Hesperidin	0.505	31.481	**0.996**	-1.715	No	No	0.211	0.525	2.506	No
Ethyl p-methoxycinnamate	**1.563**	**97.039**	-0.057	**0.111**	No	No	**0.809**	0.997	2.127	No
Levofloxacine	**1.365**	**97.397**	-0.028	-0.792	No	No	0.414	0.965	2.59	Yes

Caco2, colorectal adenocarcinoma; VDss, volume distribution; BBB, blood-brain barrier; CYP, cytochrome 450; LD50, lethal dose 50.

Table 2. The table that shows the prediction of drug similarity results .

Compounds	Muegge	Egan / Veber			Lipinski			Ghose		
	XLOGP	WLOGP	TPSA	Rot Bond	HBA	HBD	MLOGP	MW	WLOGP	MR
Eugenol	2.27	2.13	29.46	3	2	1	2.01	**164.2**	2.13	49.06
Cinnamaldehyde	1.9	1.79	17.07	2	1	0	2.01	**132.16**	1.79	41.54
Curcumin	3.2	3.15	93.06	8	6	2	1.47	368.38	3.15	102.8
Hesperidin	**-0.14**	**-1.48**	**234.29**	7	**15**	**8**	-3.04	**610.56**	**-1.48**	**141.41**
Ethyl p-methoxycinnamate	3.15	2.16	35.53	5	3	0	2.16	206.24	2.16	58.73
Levofloxacine	-0.39	1.2	75.01	2	6	1	0.98	361.37	1.2	101.83

TPSA, topography polar surface area; HBA, hydrogen bond acceptor; hydrogen bond donor; MW, molecular weight; MR, molar refraction.

GyrA and *gyrB* Active Site Discovery, Ligand Validation, Molecular Docking

Discovery of the *gyrA* and *gyrB* active site, ligand validation, and molecular docking using MVD software (Molegro® Virtual Docker version 5.5).[41] The compound to be stocked is stored in 3D geometry with the lowest value MMFF94 mode energy pool.[42] The best active site was obtained by attaching a control compound (levofloxacin) to *gyrA* and *gyrB* to obtain the least minimum energy score. The binding site molecular docking was validated as an antibacterial by redocking the control compound (levofloxacin) on the active site of *gyrA* and *gyrB*. The acceptance criteria were set with an RMSD value ≤ 2.0 Å.[41] Evaluation is carried out using the Moldock score. The smaller the score obtained, the more stable the binding between the ligand and the receptor.[39] The Moldock score is the total energy of interaction of external and internal ligands. External ligand interactions are a sum of the energies of protein-ligand interactions and consistent cofactor-ligand interactions.

RESULTS

ADMET Prediction

The results of ADMET prediction indicate that the compounds eugenol, cinnamaldehyde, and Ethyl p-methoxycinnamate are likely to be well absorbed in the digestive tract due to their Caco2 permeability greater than 8×10^{-6} cm/s. Caco2 cell lines are epithelial cancer cells from the human colon and rectum, consisting of a single layer, serving as a model for in vitro digestive mucosa to predict the absorption of orally administered drugs.[38] The predictions also show that the Caco2 permeability of eugenol, cinnamaldehyde, and Ethyl p-methoxycinnamate is greater than that of levofloxacin and even Levofloxacin. Hesperidin has the lowest predicted absorption compared to other compounds and the control. The results of the volume distribution prediction indicate that hesperidin has a higher concentration in tissues compared to plasma, while curcumin is more distributed in plasma, although not as much as Levofloxacin. Eugenol and cinnamaldehyde are likely to penetrate the blood-brain barrier as they have a log P value > 0.45 L/kg. Curcumin and hesperidin have a very low likelihood of penetrating the blood-brain barrier because they have a log P value < -0.15 L/kg, as well as the control compound.

The prediction results indicate that all compound metabolisms do not inhibit CYP 2D6 and CYP 3A4. CYP 2D6 and CYP 3A4 are the two most abundant isoforms of cytochrome P450, where approximately 80% of drugs are metabolized by them.[20,38] Only curcumin can inhibit CYP 3A4. The prediction of the total clearance rate of compounds in the body is a combination of hepatic clearance, which includes liver metabolism, biliary excretion, and renal clearance.[38] The greater the total clearance, the faster the compound will be eliminated from the body. Clearance rate values are needed to determine the average dose and estimate the duration of the drug in the body. The results of the total clearance rate prediction show that all compounds except ethyl para-methoxycinnamate have lower values compared to the control, indicating that they are expected to stay in the body longer. Based on toxicity predictions using the pkCSM software, these compounds are relatively safe for the liver and do not cause toxic effects. Maximum dose predictions based on body weight per day have also been obtained, serving as further safety references.

Drug similarity prediction

Predictions to assess compound similarity for drug functionality are conducted based on various criteria commonly used, following the principles of Muegge, Egan, Veber, Lipinski, and Ghose.[37] Molecular weight is one of the requirements specified by Lipinski, Ghose, and Muegge. Eugenol and Cinnamaldehyde do not meet Muegge's criteria due to their molecular weight being too light, i.e., less than 200 grams/mol.[63] Ghose also rejects Cinnamaldehyde because its molecular weight is less than 160 grams/mol.[43] Hesperidin fails to meet the criteria of Muegge, Lipinski, and Ghose because its molecular weight exceeds the maximum limits of 600, 500, and 480 grams/mol, respectively. Egan, Veber, and Muegge criteria do not qualify for hesperidin because it exceeds the maximum limits for TPSA, namely 131.6, 140, and 150.

Hesperidin also surpasses the constraints set by Muegge's criteria, with the maximum hydrogen acceptors exceeding 10 and donors less than 5. Hesperidin's molar refractivity also exceeds Ghose's limit of 130, as well as WLogP, which should be less than -0.4.

Three-Dimensional Structure of the Indonesian *gyrA H. pylori* Strain

The three-dimensional shape of *gyrA* was obtained through prediction using SWISS-MODEL.[35] *GyrA* is composed of two side functions consisting of groups β strands and α helices. Two strands α helices are arranged lengthwise with notches at the ends and the other strand forms a triangle-like shape. A single strand α helices connects the two at the end. The five strands of the group α helices are on the middle side with two short strands β sheets inedged. A strand of α helices seemed to dangle outwards from this group. The β strands group is on the middle side consisting of five β sheets with two short α helices as a link at the ends. *GyrA* has a group of β strands on the other end side consisting of twenty-three β sheets making a ball formation that has space in the middle.

The cavity formed with Molegro Virtual Docker (MVD) Ver.5.5 is a binding site location that can be used as a reference for the molecular docking process.[44] The five reference positions have volumes of 745.472, 252.928, 104.448, 89.6, and 75.264 with surface areas of 2204.16, 788.48, 298.24, 313.6, and 288. Molecular docking of the *gyrA* at the five reference positions resulted in scores of -107.176, -102.833, -89.6367, -92.3519, and -87.1997. The best position (score -107.176) is used as a reference for anchoring.

Molecular Docking Studies on *gyrA*

The grid box for the binding site is positioned on the X-axis at -26.23 Å, on the Y-axis at 14.55 Å, and the Z-axis at 51.75 Å. The Levofloxacin docking process at this position yielded the best score. The results of the redocking process for the validation of the binding site positions obtained an RMSD value of 0.13 Å, as shown in Figure 2. These results indicate that the method is valid for use in docking studies, as the RMSD value is less than 2 Å.[41]

The docking of various compounds on *gyrA* results in hydrophobic interactions, hydrogen bond interactions, and electrostatics. Levofloxacin has halogen bonds as a differentiator from other compounds. The lowest scores were obtained for curcumin and hesperidin, while cinnamaldehyde, ethyl para methoxycinnamate, and eugenol produced higher scores than levofloxacin. The results of attaching levofloxacin to *gyrA* showed an average Moldock score of -85.60964 kcal/mol. Hydrogen bond interactions consist of conventional, carbon-hydrogen, and Pi-donor hydrogen bonds. Hydrophobic interactions consist of Amide-Pi Stacked, Pi-alkyl, and Alkyl. Electrostatic bonds are of the Pi-anion and Pi-cation types.

Conventional hydrogen bonds are obtained at amino acid residues A: Cys 810, A: Glu 814, and A: Pro 811 with distances 2.84 Å, 2.77 Å, 1.65 Å. Carbonic hydrogen bonds are obtained at amino acid residues A: Arg 580, A: Glu 813, A: Glu 814, A: Gly 534, A: Ile 599, A: Lys 535, A: Lys 811, A: Lys 812, A: Phe 545, and A: Pro 810 with distance 2.63 Å, 2.27 Å, 2.41 Å, 2.86 Å, 2.33 Å, 2.81 Å, 2.44 Å, 2.56 Å, 2.73 Å, 2.74 Å. Pi-donor hydrogen bonds are obtained at amino acid A: Glu 814 with a distance of 2.94 Å. Stacked Amide-Pi type hydrophobic bonds are formed on amino acid residues A: Leu 536 and A: Lys 535 with distances 4.35 Å and 4.35 Å. Alkil-type hydrophobic bonds are formed on amino acid residues A: Ile 546, A: Leu 536, A: Pro 810, and A: Pro 811 with distance 4.68 Å, 4.85 Å. 4.73 Å, 5.31. Pi-alkyl type hydrophobic bonds are formed on amino acid residues A: Pro 810, A: Ile 546, A: Phe 549, A: Tyr 525, and A: Tyr 805 with distance 5.34 Å, 5.45 Å, 3.2 Å, 5.42 Å, 5.42 Å. Pi-nation electrostatic interactions are obtained at amino acid residues A: Arg 580 and A: Arg 778 with distances of 3.42 Å, and 4.69 Å. Pi-anion electrostatic interactions are obtained at amino acid residues A: Glu 547 with a distance of 2.94 Å. Halogen bonds are obtained at amino acid residues B: Glu 812, A: Glu 813, A: Glu 814, A: Ile 599, and A: Leu 536 with distance 3.352 Å, 3.42 Å, 3.59 Å, 2.93 Å, 2.63 Å.

Hesperidin exhibited hydrophobic, hydrogen bonding, and electrostatic interactions with an average Moldock score of -161.4728 kcal/mol. The hydrogen bonding interactions of hesperidin include conventional hydrogen bonds, carbon-hydrogen bonds, and Pi-donor hydrogen bonds. Hydrophobic interactions consist of Pi-Pi T-shaped, Pi-Alkyl, and Alkyl bonds. The electrostatic interactions are of the Pi-cation and Pi-anion type. Conventional hydrogen bonds are obtained at amino acid residues A: Arg 580, A: Arg 778, A: Cys 809, A: Leu 536, A: Lys 811, A: Lys 812, A: Pro 810, A: Pro 811, and A: Tyr 525 with distance 2.78 Å, 1.82 Å, 2.17 Å, 1.53 Å, 2.22 Å, 2.69 Å, 1.96 Å, 1.66 Å, 1.92 Å. Carbonic hydrogen bonds are obtained at amino acid residues A: Arg 580, A: Glu 547, A: Glu 812, A: Glu 813, A: Glu 814, A: Ile 599, A: Lys 535, A: Met 583, and A: Pro 811 with distance 2.63 Å, 1.87 Å, 2.53 Å, 2.65 Å, 2.76 Å, 2.33 Å, 1.74 Å, 2.22 Å, 2.49 Å. Pi-donor type hydrogen bonds are obtained at amino acid residues A: Ala 705 with a distance of 2.7 Å. Alkyl-type hydrophobic bonds are formed on amino acid residues A: Ile 546, A: Ala 705, A: Cys 809, A: Ile 546, A: Lys 518, A: Lys 812, and A: Pro 811 with distance 4.38 Å, 4.31 Å, 3.7 Å. 4.37 Å, 3.29 Å, 5.3 Å. Pi-alkyl hydrophobic bonds are obtained on amino acid residues A: Cys 809, A: Met 583, A: Phe 545, A: Pro 810, and A: Pro 811 with distances 5.26 Å, 5.26 Å, 4.87 Å, 3.97 Å, 4.85 Å, 4.95 Å. Pi-Pi T-shaped hydrophobic bonds are obtained on amino acid residues A: Tyr 525 and A:Tyr 805 with distance 5.14 Å, 4.88 Å. Pi-cation type electrostatic bonds are obtained at amino acid residues A: Arg 580 and A: Arg 778 with distance 4.63 Å, 4.69 Å. Pi-anion type electrostatic bonds are obtained in amino acid residues A: Glu 812 with a distance of 4.96 Å.

The molecular docking results of Curcumin to *gyrA* obtained hydrophobic interactions, hydrogen bond interactions, and electrostatics with an average moldock score value of -150.9947 kcal/mol. The hydrogen bond interaction consists of conventional hydrogen bonds and carbon-hydrogen bonds. Hydrophobic interactions consist of Pi-Pi, T-shaped, Pi-alkyl, and Alkyl ones. Electrostatic bonds are Pi-anion and Pi-cation types. Conventional hydrogen bonds are obtained at amino acid residues A: Arg 580, A: Arg 778, A: Cys 809, A: Gly 534, and A: Ile 546 with distances 2.48 Å, 1.94 A, 2.38 A, 2.64 Å, 2.29 A. Carbon hydrogen bonds are obtained in amino acid residues A: Glu 812, A: Glu 813, A: Glu 814, A: Leu 536, A: Lys 518, A: Lys 811, A: Pro 810, and A: Pro 811 with distance 2.84 Å, 2.83 Å, 2.79 Å, 2.69 Å, 2.34 Å, 2.48 Å, 2.05 Å, 2.5 Å. Alkyl-type hydrophobic bonds are formed on amino acid residues A: Met 583 with a distance of 4.25 Å. Pi-alkyl hydrophobic bonds are formed on amino acid residues A: Cys 809, A: Cys 810, A: Ile 546, A: Leu 536, A: Pro 810, A: Pro 811 and A: Tyr 805 with distance 5.22 Å, 5.41 Å, 4.83 Å, 4.95 Å, 4.68 Å, 4.24 Å, 4.31 Å. Pi-Pi T-shaped hydrophobic bonds are obtained on amino acid residues A: Phe 549 and A: Tyr 805 with distances of 5.92 Å, and 5.06 Å. Pi-cation type electrostatic interaction is obtained on amino acid residues A: Arg 778 with a distance of 4.73 Å. Pi-anion type electrostatic interaction is obtained on amino acid residues A: Glu 547 and A: Glu 813 with distances of 4.67 Å and 4.29 Å.

The molecular docking results of cinnamaldehyde on *gyrA* obtained hydrophobic interactions, hydrogen bond interactions, and electrostatics with an average moldock score value of -73.21497 kcal/mol... The hydrogen bond interaction consists of conventional hydrogen bonds and carbon-hydrogen bonds. Hydrophobic interactions consist of Pi-Pi T-shaped, Amide-Pi Stacked, and Pi-alkyl. Electrostatic interaction of Pi-cation type. Conventional hydrogen

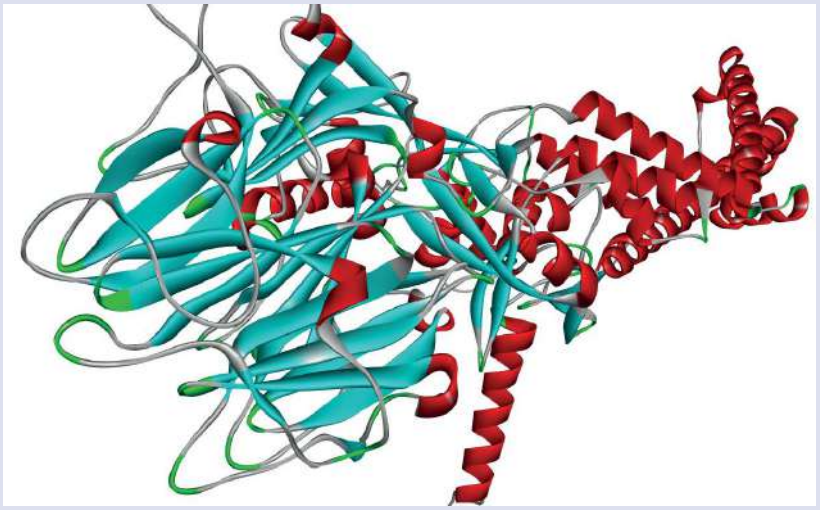

Figure 1. The three-dimensional shape of *gyrA* by SWISS-MODEL prediction. Visualization by Discovery Studio Visualizer.

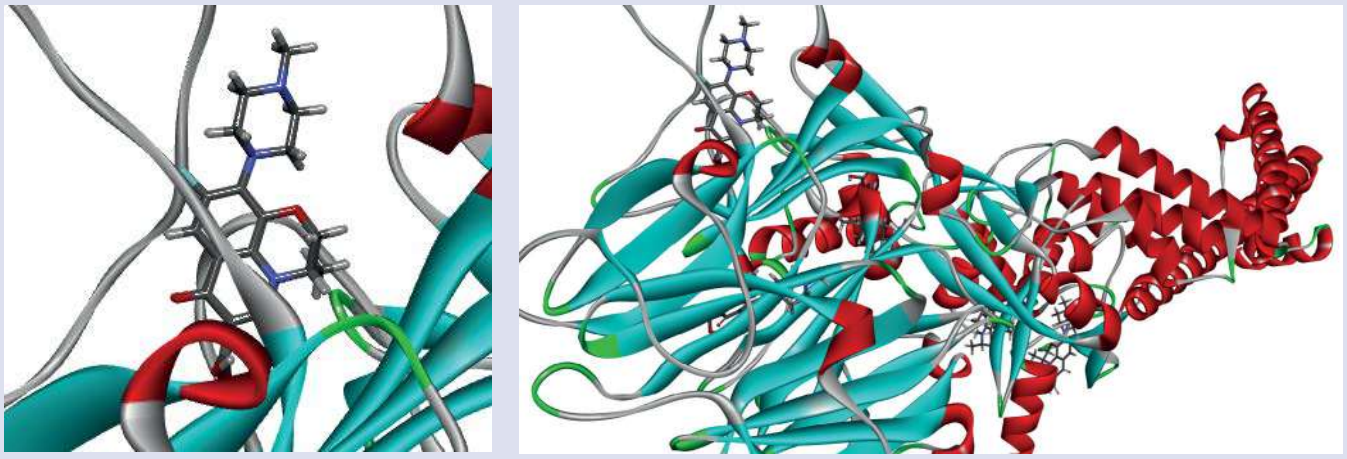

Figure 2. The figure that showing some possible reference positions for anchoring in *gyrA* (right). Comparison of re-docking results for the validation process with Molegro Virtual Docker (MVD) Ver.5.5 with RMSD 0.5 Å (left).

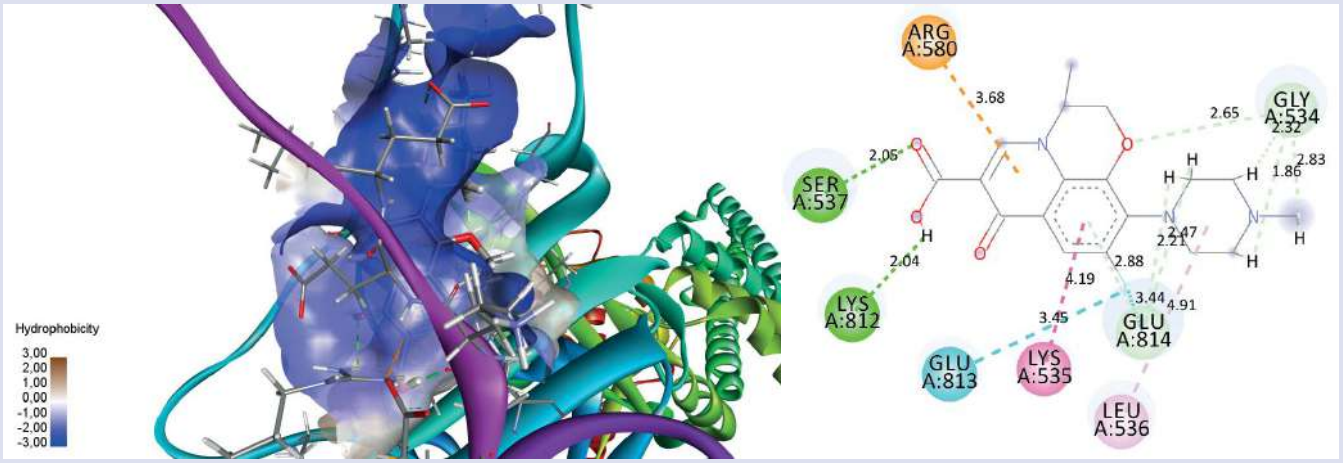

Figure 3. Molecular docking experiments targeting *gyrA* and levofloxacin. Levofloxacin interactions at the active site of *gyrA* are shown as dashed lines indicating hydrogen bonding (green), hydrophobic interaction (pink), halogen interaction (blue), and electrostatic interaction (orange) by Biovia Discovery Studio.

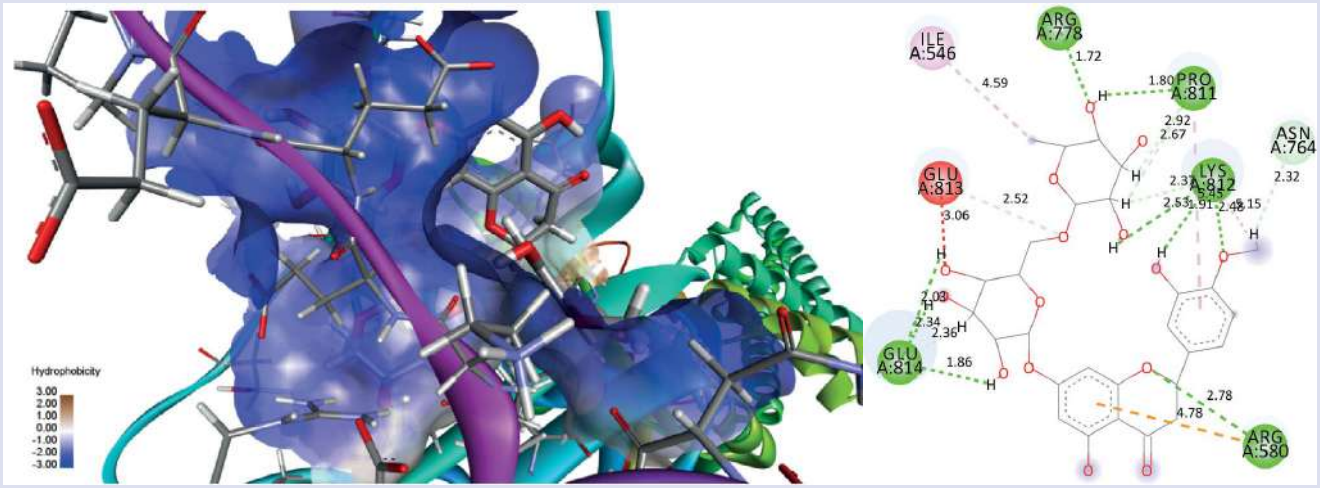

Figure 4. Molecular docking experiments targeting *gyrA* and hesperidin. Hesperidin interactions at the active site of *gyrA* are shown as dashed lines indicating hydrogen bonding (green), hydrophobic interaction (pink), and electrostatic interaction (orange) by Biovia Discovery Studio.

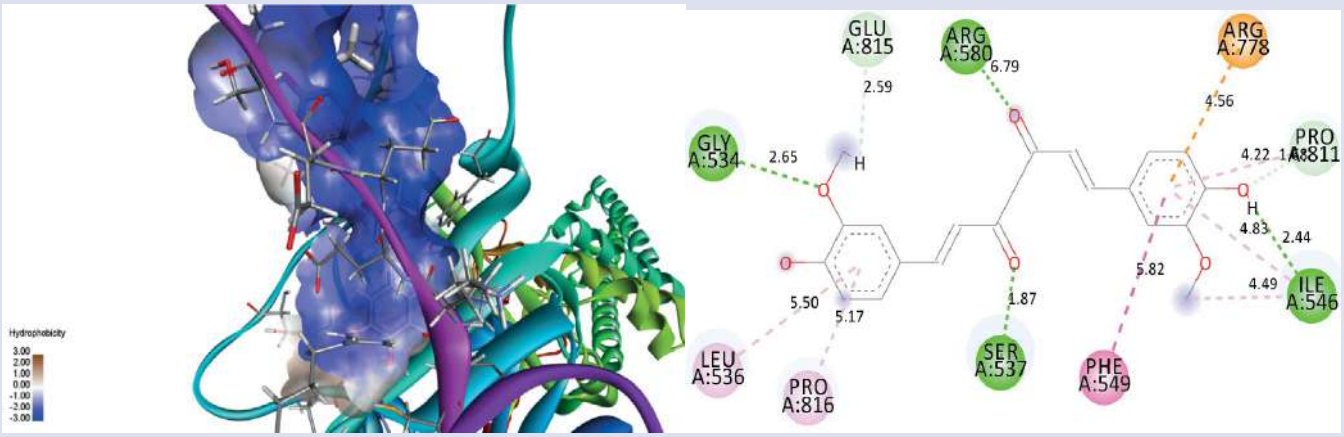

Figure 5. Molecular docking experiments targeting *gyrA* and curcumin (white). Curcumin interactions at the active site of *gyrA* are shown as dashed lines indicating hydrogen bonding (green), hydrophobic interaction (pink), and electrostatic interaction (orange) by Biovia Discovery Studio.

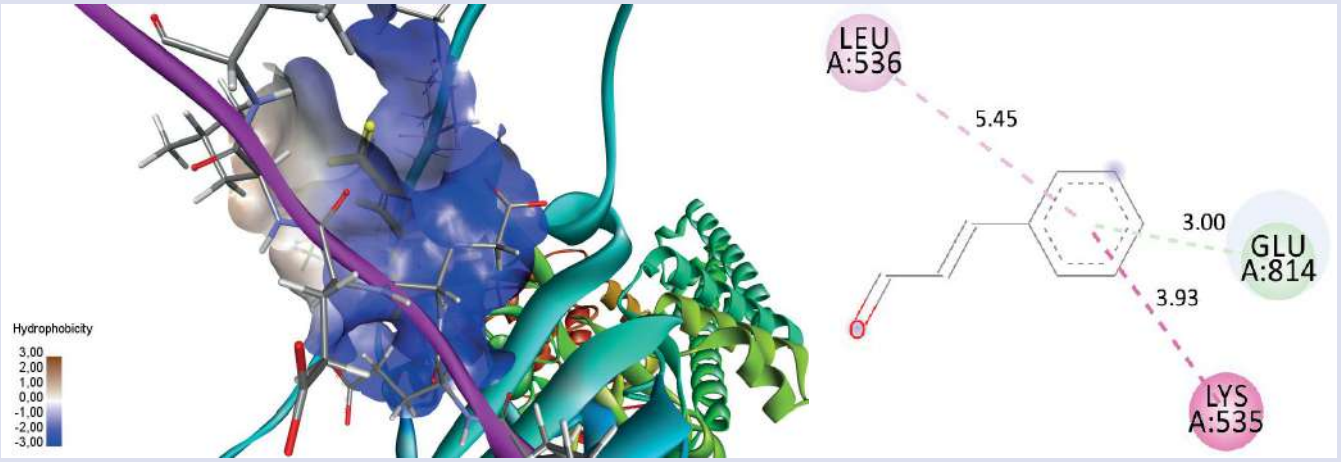

Figure 6. Molecular docking experiments targeting *gyrA* and cinnamaldehyde. Cinnamaldehyde interactions at the active site of *gyrA* are shown as dashed lines indicating hydrogen bonding (green), hydrophobic interaction (pink), and electrostatic interaction (orange) by Biovia Discovery Studio.

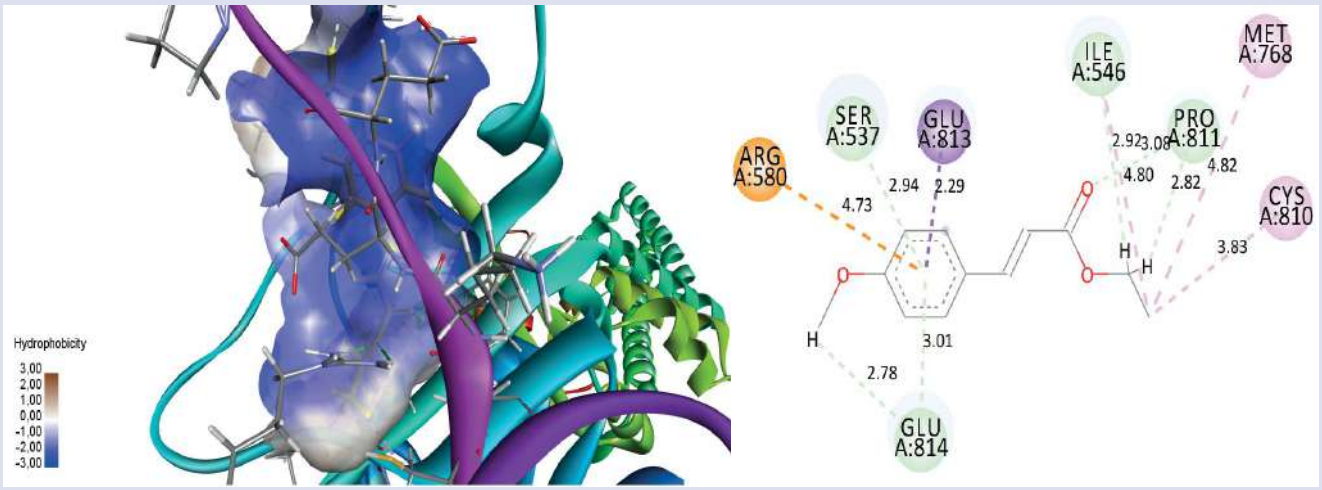

Figure 7. Molecular docking experiments targeting *gyrA* and ethyl para methoxycinnamate. Ethyl para methoxycinnamate interactions at the active site of *gyrA* are shown as dashed lines indicating hydrogen bonding (green), hydrophobic interaction (pink), and electrostatic interaction (orange) by Biovia Discovery Studio.

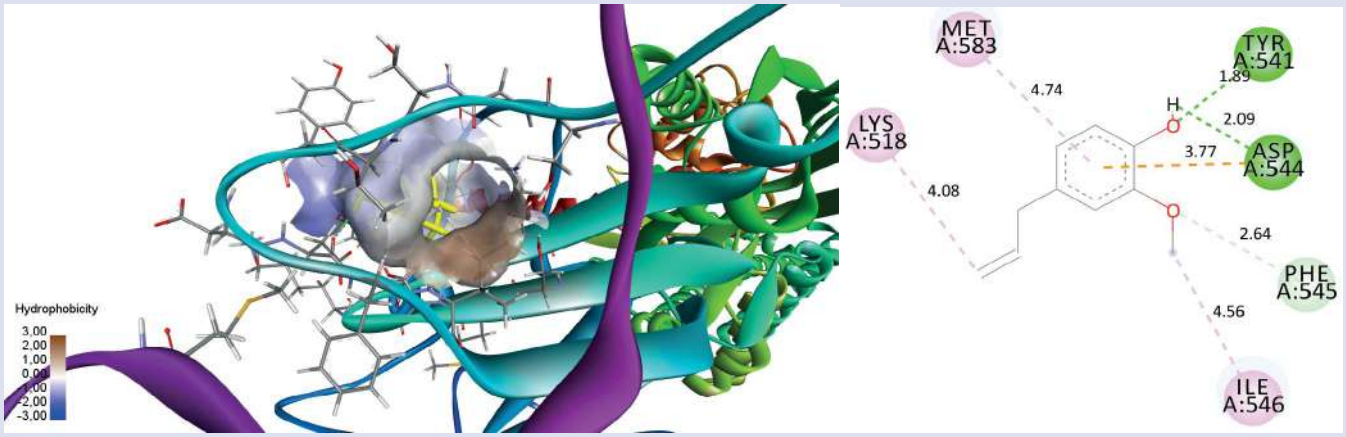

Figure 8. Molecular docking experiments targeting *gyrA* and eugenol (yellow). Eugenol interactions at the active site of *gyrA* are shown as dashed lines indicating hydrogen bonding (green), hydrophobic interaction (pink), and electrostatic interaction (orange) by Biovia Discovery Studio.

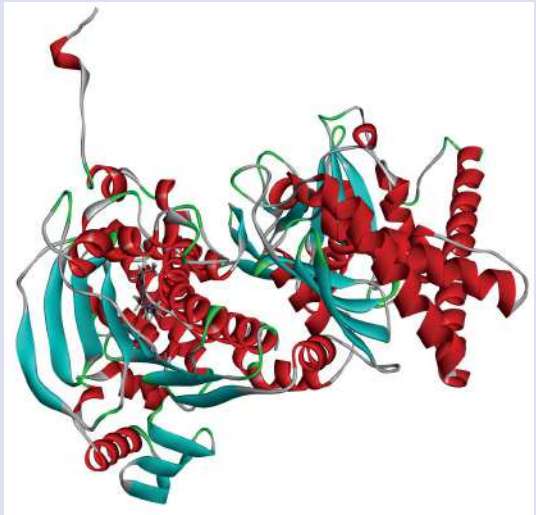

Figure 9. The three-dimensional shape of *gyrB* by SWISS-MODEL prediction. Visualization by Discovery Studio Visualizer.

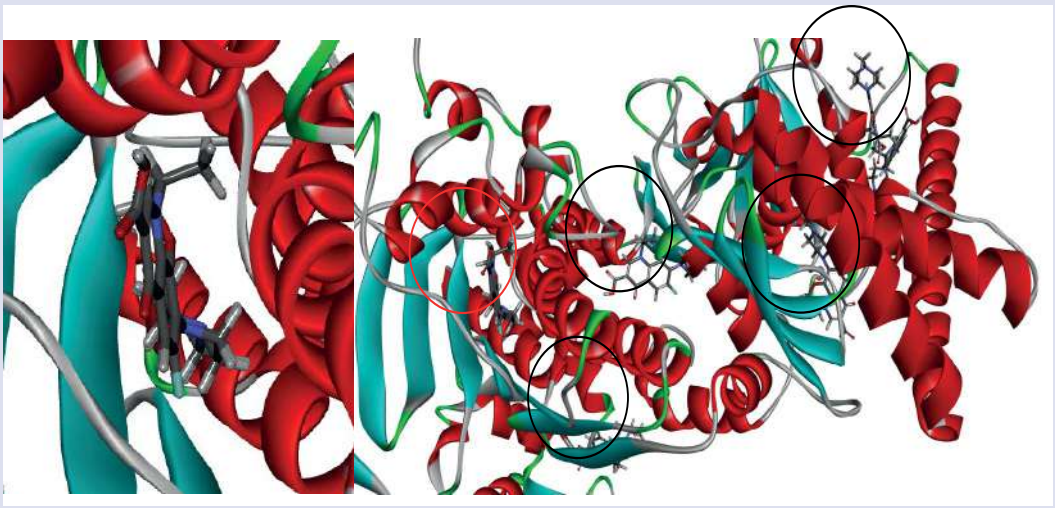

Figure 10. This is a figure that shows some possible reference positions for anchoring in gyrB (right). Comparison of re-docking results for the validation process with Molegro Virtual Docker (MVD) Ver.5.5 with RMSD 0.0024 Å (left).

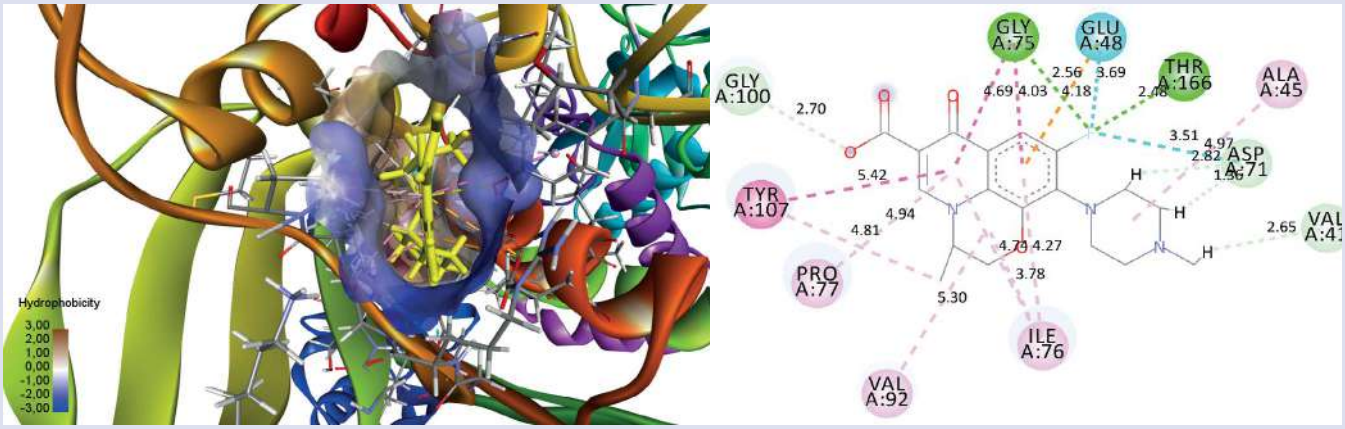

Figure 11. Molecular docking experiments targeting *gyrB* and levofloxacin (yellow). The levofloxacin interactions at the active site of *gyrB* are shown as dashed lines indicating hydrogen bonding (green), hydrophobic interaction (pink), and halogen interaction (blue). and electrostatic interaction (orange) by Discovery Studio Visualizer.

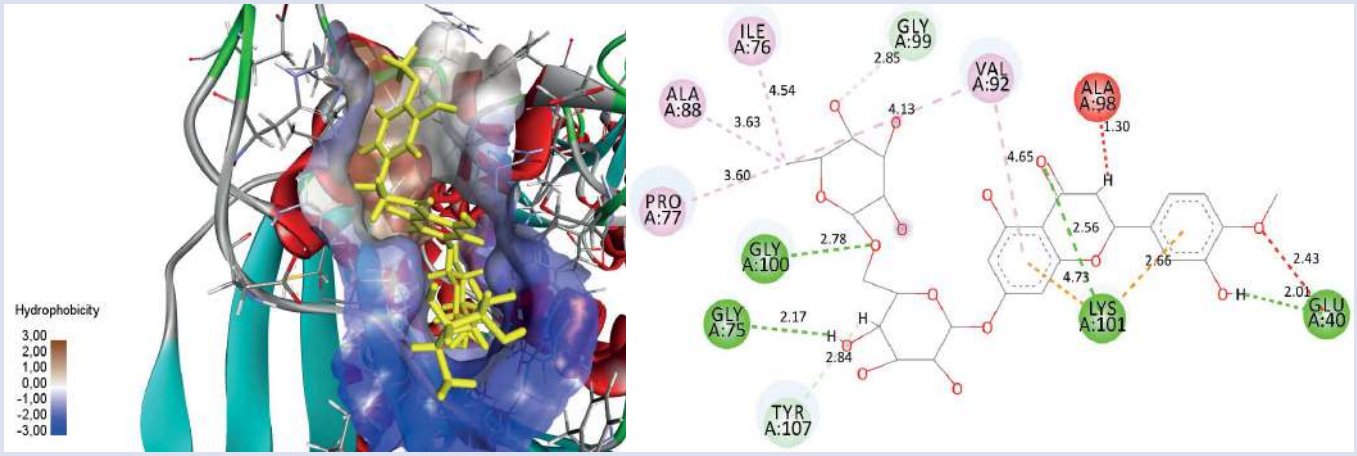

Figure 12. Molecular docking experiments targeting *gyrB* and hesperidin (yellow). The hesperidin interactions at the active site of *gyrB* are shown as dashed lines indicating hydrogen bonding (green), hydrophobic interaction (pink), and electrostatic interaction (orange) by Discovery Studio Visualizer.

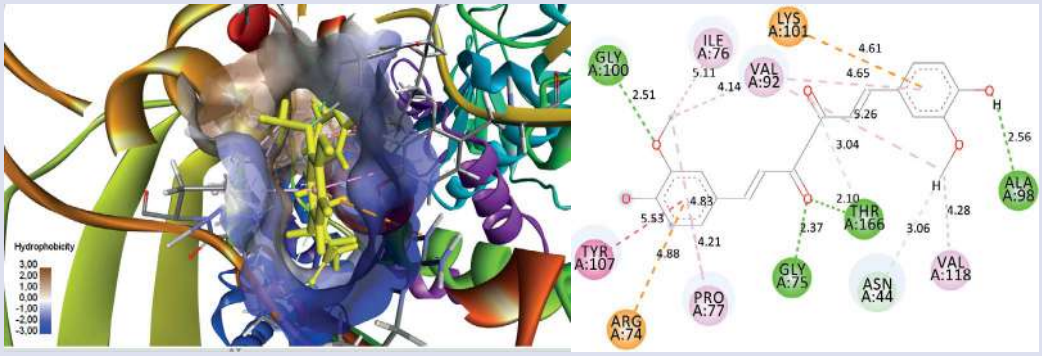

Figure 13. Molecular docking experiments targeting *gyrB* and curcumin (yellow). The curcumin interactions at the active site of *gyrB* are shown as dashed lines indicating hydrogen bonding (green), hydrophobic interaction (pink), and electrostatic interaction (orange) by Discovery Studio Visualizer.

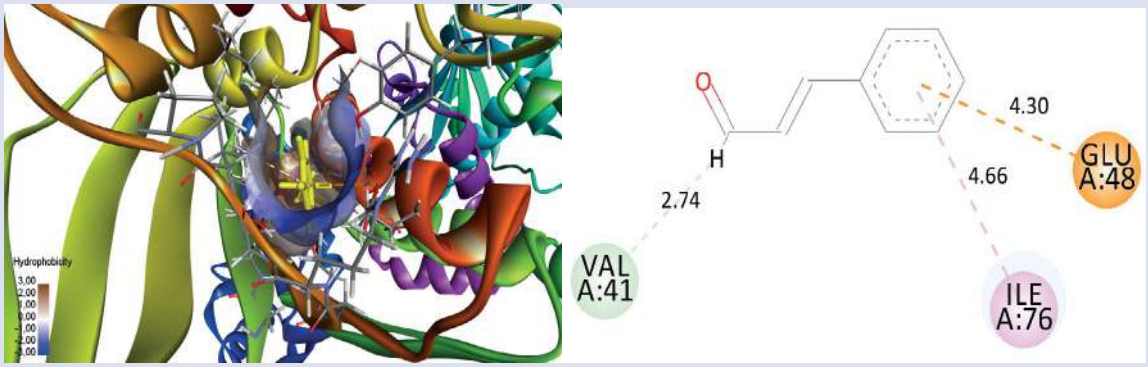

Figure 14. Molecular docking experiments targeting *gyrB* and cinnamaldehyde (yellow). The cinnamaldehyde interactions at the active site of *gyrB* are shown as dashed lines indicating hydrogen bonding (green), hydrophobic interaction (pink), and electrostatic interaction (orange) by Discovery Studio Visualizer.

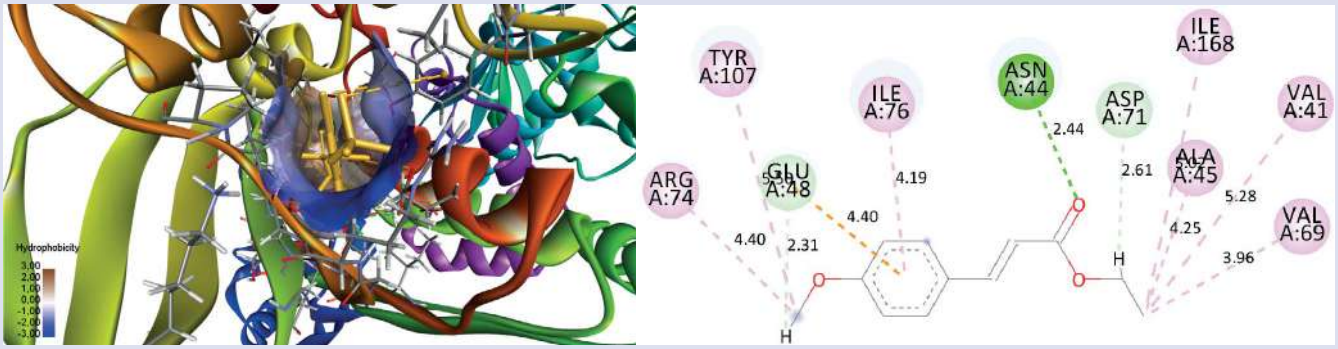

Figure 15. Molecular docking experiments targeting *gyrB* and ethyl p-methoxycinnamate (yellow). The ethyl p-methoxycinnamate interactions at the active site of *gyrB* are shown as dashed lines indicating hydrogen bonding (green), hydrophobic interaction (pink), and electrostatic interaction (orange) by Discovery Studio Visualizer.

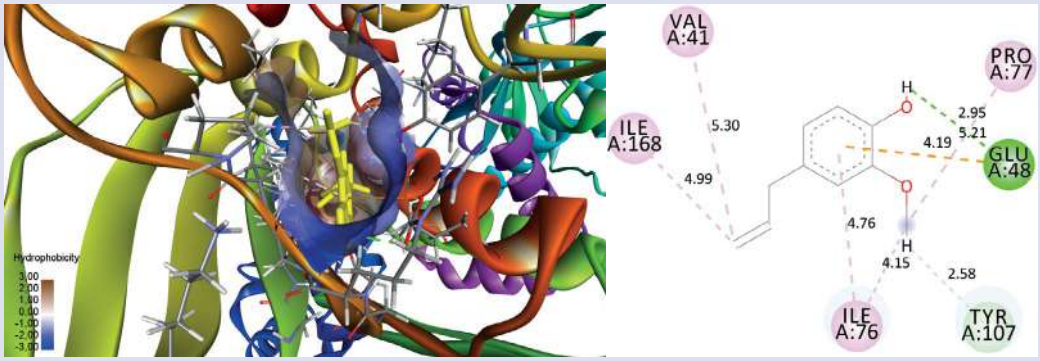

Figure 16. Molecular docking experiments targeting *gyrB* and eugenol (yellow). The eugenol interactions at the active site of *gyrB* are shown as dashed lines indicating hydrogen bonding (green), hydrophobic interaction (pink), and electrostatic interaction (orange) by Discovery Studio Visualizer.

bonds are obtained at amino acid residues A: Arg 778 with a distance of 2.8 Å. Pi-donor type hydrogen bonds are obtained in amino acid residues A: Glu 814 with a distance of 3 Å. Carbon hydrogen bonds are obtained in amino acid residues A: Ile 546 and A: Lys 518 with distance 3 Å and 2.5 Å. Pi-alkyl type hydrophobic interactions are formed on amino acid residues A: Ala 705, A: Ile 546, A: Leu 536, and A: Pro 810 with distance 4.06 Å, 4.25 Å, 5.45 Å, 3.82 Å. Amide-Pi Stacked hydrophobic interactions are formed on amino acid residues A: Leu 536 and A: Lys 535 with distances 3.95 Å, and 3.93 Å. Pi-Pi T-shaped hydrophobic interactions are formed on amino acid residues A: Phe 549 with a distance of 5.04 Å. Pi-cation type electrostatic interaction is formed on amino acid residues A: Arg 580 with a distance of 4.37 Å.

The molecular docking results of ethyl para methoxycinnamate on *gyrA* obtained hydrophobic interactions, hydrogen bond interactions, and electrostatics with the average Moldock score value is -99.52707 kcal/mol. The hydrogen bond interaction consists of conventional hydrogen bonds and carbon-hydrogen bonds. Hydrophobic interactions consist of Amide-Pi Stacked, Pi-sigma, Pi-alkyl, and alkyl. Conventional hydrogen bonds are obtained at amino acid residues A: Ala 705 (2.37 Å), A: Arg 778 (2.19 Å), and A: Cys 809 (2.45 Å). Carbon hydrogen bonds are obtained in amino acid residues A: Glu 814 (2.65 Å), A: Gly 534 (2.73 Å), A: Ile 546 (3.02 Å), A: Lys 812 (3.02 Å), A: Pro 810 (2.36 Å), and A: Pro 811 (2.82 Å). Alkyl-type hydrophobic interactions are obtained on amino acid residues A: Ala 705 (3.54 Å), A: Cys 810 (3.81 Å), A: Ile 546 (4.41 Å), and A: Leu 536 (4.54 Å). Pi-alkyl-type hydrophobic interactions are obtained on amino acid residues A: Phe 545 (4.66 Å) and A: Phe 549 (4.32 Å). Amide-Pi Stacked hydrophobic interaction is obtained on amino acid residues A: Lys 535 and A: Lys 536 with their respective distances of 3.83 Å. Pi-sigma type hydrophobic interaction is obtained on amino acid residues A: Glu 813 with a distance of 2.28 Å. Pi-cation type electrostatic interaction is formed on amino acid residues A: Arg 580 with a distance of 4.42 Å. Pi-anion type electrostatic interactions are formed at amino acid residues A: Glu 812 with a distance of 4.01 Å.

The molecular docking result of Eugenol to *gyrA* obtained hydrophobic interactions, hydrogen bond interactions, and electrostatics with the average Moldock score value is -79.6928 kcal/mol. Hydrogen bond interactions consist of conventional hydrogen bonds, carbon-hydrogen bonds, and hydrogen Pi-donors. Hydrophobic interactions consist of Amide-Pi Stacked, Pi-Pi T-shaped, Pi-alkyl, and alkyl. Conventional hydrogen bond interactions are obtained at amino acid residues A: Arg 580 (2.89 Å), A: Cys 809 (1.84 Å), A: Glu 813 (2.37 Å), and A: Ile 546 (2.3 Å). The interaction of carbon-hydrogen bonds is obtained in amino acid residues A: Glu 547 (2.5 Å), A: Glu 814 (2.36 Å), A: Glu 547 (2.5 Å), A: Gly 534 (2.89 Å), A: Lys 535 (2.2 Å), and A: Phe 545 (2.64 Å). Pi-donor hydrogen bond interaction is obtained at amino acid residues A: Ile 546 with a distance of 2.9 Å. Alkyl-type hydrophobic interactions are present in amino acid residues A: Ile 546 (4.56 Å), A: Ile 599 (4.39 Å), A: Pro 810 (3.91 Å), A: Cys 809 (4.58 Å), and A: Lys 518.

Three-Dimensional Structure of the Indonesian *gyrB H. pylori* Strain

The three-dimensional shape of *gyrB* was obtained through prediction using SWISS-MODEL.[35] *GyrB* is composed of a penta dihedral with open holes at its base flanked by eight β sheets on one side and three β sheets on the other. Six α helices connect the eight β sheets to four β sheets on the inside. Five α helices connect the three β sheets to eight woven eight β sheets on the inner side. The two formations are connected by a long α of helices that form sharp notches in the shape of a pointed pentagonal peak.

The cavity formed with Molegro Virtual Docker (MVD) Ver.5.5 is a binding site location that can be used as a reference for the molecular docking process.[44] The five reference positions have volumes of 4413.44, 203.264, 125.952, 44.544, and 29.690 with surface areas of 11928.3, 573.6, 430.08, 170.24, and 102.4. Molecular docking of the *gyrA* at the five reference positions resulted in scores of -105.208, -96.8272, -123.011, -79.56, and -77.2093. The best position (score -123.011) is used as a reference for anchoring.

Molecular Docking Studies on *gyrB*

The grid box for the binding site is positioned on the X-axis at -15.98 Å, on the Y-axis at 0.76 Å, and the Z-axis at 28.51 Å. The molecular docking results of the levofloxacin in that position obtained the best score. The results of the redocking process for the validation of the binding site positions obtained an RMSD value of 0.0024 Å which can be observed in Figure 9. These results indicate that the method is valid for use as a belay test because the RMSD value is less than 2 Å.

The docking of various compounds on *gyrB* results in hydrophobic interactions, hydrogen bond interactions, and electrostatics. Levofloxacin has halogen bonds as a differentiator from other compounds. The hydrogen bond interaction consists of conventional hydrogen bonds and carbon-hydrogen bonds. Hydrophobic interactions consist of *Amide-Pi Stacked*, Pi-alkyl, and Alkyl. The electrostatic interaction obtained is of Pi-anion type. The lowest scores were obtained on curcumin and hesperidin, while cinnamaldehyde, ethyl para-methoxycinnamate, and eugenol produced higher scores than levofloxacin. The molecular docking results of levofloxacin to *gyrB* obtained an average *moldock score* value of -122.5873 kcal/mol.

Conventional hydrogen bond interactions are obtained at amino acid residues A: Asn 44 (2.56 Å), A: Gly 75 (2.52 Å), and A: Val 41 (1.68 Å). Carbon hydrogen bonds are obtained in amino acid residues A: Asn 44 (2.56 Å), A: Asp 71 (1.33 Å, 2.66 Å), A: Gly 75 (2.5 Å), A: Gly 100 (2.66 Å), A: Thr 166 (2.5 Å), A: Tyr 107 (2.66 Å), and A: Val 41 (2.67 Å). Amide-Pi Stacked hydrophobic interaction is obtained on amino acid residues A: Asn 44 and A: Gly 75 with distances 4.39 Å and 3.99 Å. Pi-pi T-shape type hydrophobic interactions are present in amino acid residues A: Tyr 107 with a distance of 5.4 Å. Pi-alkyl hydrophobic bonds are present in amino acid residues A: Ile 76 (4 Å), A: Pro 77 (4.9 Å), and A: Tyr 107 (4.8 Å). Alkyl-type hydrophobic bonds are obtained on amino acid residues A: Ala 45 (5 Å), A: Ile 76 (3.7 Å), and A: Val 92 (4.68 Å). Pi-anion type electrostatic interaction is obtained at amino acid residues A: Glu 48 with a distance of 4.2 Å. Halogen bonds are obtained in amino acid residues A: Asp 71 (3.5 Å), A: Glu 48 (3.6 Å), A: Gly 75 (2.57 Å), and A: Thr 66 (2.4 Å).

The molecular docking result of hesperidin to *gyrB* obtained hydrophobic interaction and hydrogen bond interaction with an average Moldock score value of -151.8591 kcal / mol. Neither electrostatic nor halogen interactions were found. The hydrogen bond interaction consists of conventional hydrogen bonds and carbon-hydrogen bonds. The hydrophobic interaction consists of Pi-alkyl and alkyl. Conventional hydrogen bond interactions are obtained at amino acid residues A: Ala 45 (2.09 Å), A: Arg 74 (2.58 Å), A: Asp 71 (1.52 Å), A: Glu 48 (2.54 Å), A: Gly 75 (2.8 Å), A: Gly 100 (2.73 Å), A: Asn 44 (2.7 Å), A: Lys 101 (2.82 Å), A: Tyr 107 (2.32 Å), A: Val 41 (1.62 Å), and A: Val 69 (2.46 Å). The interaction of carbon-hydrogen bonds is obtained in amino acid residues A: Arg 74 (2.94 Å), A: Asp 71 (1.52 Å), A: Gly 75 (2.2 Å), A: Gly 100 (2.7 Å), A: Ile 76 (1.95 Å), A: Lys 101 (2.84 Å), A: Pro 77 (2.77 Å), A: Thr 166 (2.36 Å), and A: Tyr 107 (2.41 Å). Alkyl-type hydrophobic interactions are obtained on amino acid residues A: Arg 74 (2.94 Å), A: Ile 76 (4.9 Å), A: Lys 101 (3.31 Å), A: Pro 77 (3.6 Å), A: Val 41 (3.83 Å), and Val 92 (4.24 Å). Pi-alkyl hydrophobic interactions are obtained at amino acid residues A: Ile 76 (4.17 Å), A: Pro 77 (4.17 Å), A: Lys 101 (5.1 Å), A: Tyr 107 (4.17 Å), and A: Val 92 (5.25 Å). Pi-cation type electrostatic interaction is obtained at amino acid residues A: Lys 101 with a distance of 4 Å.

The molecular docking result of curcumin to *gyrB* obtained hydrophobic interactions, hydrogen bond interactions, and electrostatic interactions with an average Moldock score value of -159.2033 kcal/mol. The hydrogen bond interaction consists of conventional hydrogen bonds and carbon-hydrogen bonds. Hydrophobic interactions consist of *Amide-Pi Stacked,* Pi-alkyl, and alkyl types. Both Pi-cation and Pi-anion-type electrostatic interactions can be found. Conventional hydrogen bond interactions are obtained at amino acid residues A: Ala 98 (1.92 Å), A: Asn 44 (2.62 Å), A: Asp 71 (2.4 Å), A: Glu 48 (2.91 Å), A: Gly 75 (2.32 Å), A: Gly 100 (2.5 V), A: Thr 166 (2.15 Å), and A: Tyr 107 (2.43 Å). The interaction of carbon-hydrogen bonds is obtained in amino acid residues A: Ala 98 (2.61 Å), A: Asn 44 (2.87 Å), A: Glu 48 (2.87 Å), A: Gly 75 (2.19 Å), A: Gly 100 (2.78 Å), A: Ile 76 (2.85 Å), A: Pro 77 (2.8 Å), A: Thr 166 (2.64 Å), and A: Tyr 107 (2.62 Å). Pi-alkyl type hydrophobic interactions were obtained on amino acid residues A: Ala 45 (5.39 Å), A: Ala 98 (4.75 Å), A: Ile 76 (5.11 Å), A: Pro 77 (4.29 Å), A: Tyr 107 (4.81 Å), A: Val 91 (5.06 Å), and A: Val 92 (5.07 Å). Alkyl-type hydrophobic interactions were found in amino acid residues A: Ala 98 (4.75 Å), A: Arg 74 (3.6 Å), A: Ile 76 (4.84 Å), A: Ile 168 (3.89 Å), A: Pro 77 (4.05 Å), A: Val 91 (4.46 Å), and A: Val 92 (4.18 Å). The hydrophobic interaction of the Amide-Pi Stacked type was obtained on amino acid residues A: Ala 45 and A: Asn 44 with distances of 4.71 Å. Electrostatic interaction of Pi-cation type was obtained on amino acid residues A: Arg 74 and A: Lys 101 with distances of 4.62 Å and 5.03 Å, while Pi-anion type was found on amino acid residues A: Glu 48 with a distance of 4.26 Å.

The molecular docking result of cinnamaldehyde to *gyrB* obtained hydrophobic interactions, hydrogen bond interactions, and electrostatic interactions with an average Moldock score value of -73.81889 kcal/mol. The interaction of hydrogen bonds is only the type of carbon-hydrogen bond found in amino acid residues A: Arg 74 and A: Val 41 with distances of 2.83 Å and 2.68 Å. Hydrophobic interactions are also only obtained in Pi-alkyl types obtained in amino acid residues A: Ile 76 with a distance of 4.67 Å. Electrostatic interaction of Pi-anion type is obtained in amino acid residues A: Glu 48 with a distance of 4.25 Å.

The molecular docking result of Ethyl Para-methoxycinnamate to *gyrB* obtained hydrophobic interactions, hydrogen bond interactions, and electrostatic interactions with an average Moldock score value of -108.9359 kcal/mol. The hydrogen bond interaction consists of conventional hydrogen bonds and carbon-hydrogen bonds. Hydrophobic interactions consist of *Amide-Pi Stacked,* Pi-alkyl, and alkyl types. The electrostatic interaction obtained is only of the Pi-anion type. Conventional hydrogen bond interactions are obtained at amino acid residues A: Arg 74 and A: Asn 44 with distances of 2.8 Å and 2.3 Å. The hydrogen bond interaction of carbon is obtained in amino acid residues A: Asp 71 (2.75 Å), A: Glu 48 (2.6 Å), A: Gly 75 (2.1 Å), A: Pro 77 (2.18 Å), A: Thr 166 (2.78 Å), A: Tyr 107 (2.67 Å), and A: Val 41 (2.55 Å). The hydrophobic interaction of Pi-alkyl type is found in amino acid residues A: Tyr 107 with a distance of 5.32 Å. Hydrophobic interactions of alkyl types are obtained in amino acid residues A: Ala 45 (4.2 Å), A: Arg 74 (4.16 Å), A: Ile 168 (4.8 Å), A: Ile 76 (5.1 Å), A: Val 41 (5.27 Å), and A: Val 69 (4.83 Å). Amide-Pi Stacked hydrophobic interactions are found in amino acid residues A: Ala 45 (5.49 Å), A: Asn 44 (5.49 Å), A: Gly 75 (4.2 Å), and A: Pro 77 (3.8 Å). Pi-anion type electrostatic interaction is obtained at amino acid residue A: Glu 48 with a distance of 4.27 Å.

The molecular docking result of Eugenol to *gyrB* obtained hydrophobic interactions, hydrogen bond interactions, and electrostatic interactions with an average Moldock score value of -80.1974 kcal/mol. The hydrogen bond interaction consists of conventional hydrogen bonds and carbon-hydrogen bonds. Hydrophobic interactions consist of Amide-Pi Stacked, Pi-alkyl, and alkyl types. The electrostatic interaction obtained is only of the Pi-anion type. Conventional hydrogen bond interactions are obtained at amino acid residues A: Asp 71 (2.2 Å), A: Glu 48 (2.94 Å), and A: Thr 166 (1.9 Å). The interaction of carbon-hydrogen bonds is obtained in amino acid residues A: Asp 71 (2.28 Å), A: Glu 48 (2.6 Å), A: Gly 75 (2.73 Å), A: Thr 166 (2.8 Å), A: Tyr 107 (2.58 Å), A: Val 41 (2.2 Å), and A: Val 69 (2.7 Å). Alkyl-type hydrophobic interactions are found in amino acid residues A: Ala 45 (4.4 Å), A: Arg 74 (4.9 Å), A: Ile 76 (5 Å), A: Ile 168 (4.4 Å), A: Pro 77 (5.2 Å), A: Val 41 (5.3 Å), and A: Val 69 (4.6 Å). The hydrophobic interaction of Pi-alkyl type was obtained at amino acid residues A: Ile 76 with a distance of 5.2 Å. Hydrophobic interactions of the Amide-Pi Stacked type are found in amino acid residues A: Ala 45 and A: Asn 44 with the same distance of 4.5 Å. Pi-anion type electrostatic interaction is found in amino acid residues A: Glu 48 with a distance of 3.98 Å.

DISCUSSION

The results of molecular docking show that curcumin and hesperidin are compounds that have the most potential as anti-*H. pylori*. This is because the Moldock score produced by curcumin and hesperidin from the molecular docking process on *gyrA* and *gyrB* is better than the control compound (levofloxacin). Another study also mentioned that hesperidin also had a better docking score than control compounds as a result of molecular docking in human serum albumin (HSA) to treat digestive disorders.[45] Molecular docking of hesperidin in the NF-κB p50 DNA binding site also resulted in the best docking score compared to other compounds in treating anorexia.[46] Both studies also aimed to reduce symptoms in digestive disorders but with different target causes. The docking score of hesperidin in both studies was also better than the control compound. This suggests that hesperidin binds more easily to drug targets. Molecular docking of curcumin in the Eaph1 and Eaph2 virulence systems of Staphylococcus aureus also yielded the best values.[47] Curcumin also provides the best results when molecular docking is done on β-Lactamase, Penicillin Binding Protein 2a (PBP2a), Dihydrofolate Reductase (DHFR), including DNA gyrase.[48] Both studies were also carried out by molecular docking to obtain the potential of various compounds as antibacterial but with different bacterial targets. Nevertheless, curcumin still has the best docking score. The docking score of curcumin on DNA gyrase is also best even in different bacteria. These results show that curcumin has great potential as an antibacterial. The results of molecular docking in this study have shown that hesperidin and curcumin have scope to replace commercial drugs for *H. pylori*. Moldock scores that are more negative on curcumin and hesperidin make both compounds interact and bind more easily with *gyrA* and *gyrB*.[49]

Curcumin and ethyl para-methoxycinnamate meet all drug similarity requirements. This has been proven through screening based on the principles of Muegge, Egan, Veber, Lipinski, and Ghose who passed both. Effective and reliable virtual screening through the Curcumin Chalcone Derivatives Database (CCDD) shows that curcumin is indeed viable as a medicine.[50] Another study mentioned Curcumin also meets the drug requirements for antibacterial discovery *in silico* as an inhibitor of the *AcrB* protein that carries the gene efflux pump inhibitor *E. coli*.[51] Curcumin also meets the drug requirements to obtain antibacterial Staphylococcus aureus.[48] Both studies also used the same software, SwissADME.[37] The advantage of this study is that we used all categories of drug requirements criteria, not only using Lipinski requirements to make the results more valid and reliable.[52-53] Research on ethyl para-methoxycinnamate through *in silico* assays to date has never existed. This research provides a discourse that can be used in conducting ethyl para-methoxycinnamate studies *in silico*. Ethyl para-methoxycinnamate from *Kaempferia galanga L. (Zingiberaceae)* as one of the rich biodiversity of Indonesia and Asia still has many opportunities to be used as a medicinal compound.[54] Thus, it is clear that in terms of drug similarity curcumin and ethyl para-methoxycinnamate have potential as a drug.

Curcumin and hesperidin are expected to last longer in the stomach so that they will have longer interactions with *H. pylori* as a therapeutic target bacterium. This can be seen in the results of ADMET predictions that hesperidin is poorly absorbed and can accumulate in tissues, allowing for more significant interactions with *H. pylori* in the digestive mucosa.[55] This condition can be attributed to the relatively larger size and molecular weight of hesperidin, regardless of its chemical structure.[56] Other studies have shown that hesperidin is also more difficult to absorb through digestion. However, this cannot exclude hesperidin as one of the compounds that have the potential to be antibacterial.[57] Several other studies have also shown that ADMET predictive curcumin still meets the requirements as a drug. Many studies are done to explore various functions of curcumin on various therapeutic targets including antibacterial.[58] Various studies were also conducted *in silico*, one of which was predicting ADMET. Thus, it is clear that both curcumin and hesperidin through ADMET prediction will be able to interact for a long time with *H. pylori* and do not cause toxic effects for humans so they can be used as anti-*H. pylori*.

The results of this study have obtained a three-dimensional structural picture of the *gyrA* and *gyrB* of *H. pylori* specifically of the Indonesian strain. The discovery of this three-dimensional structure is very necessary for efforts to obtain the antibacterial potential of the Indonesian strain more precisely.[19] DNA gyrase structures (Topoisomerase II and IV) are widely available on database provider sites, but *H. pylori* data are sparse.[59] Further research can use the three-dimensional structure of DNA gyrase that has been formed. Research to obtain the potential of various antibacterials can also use the obtained structure. The three-dimensional structure of *H. pylori* DNA gyrase from different parts of the world is likely to be similar so it can also be used for various studies including drug discovery.

The results of this study are still a study *in silico* test of various compounds produced from Indonesian biodiversity plants that have the potential to be anti-*H. pylori*. Further research through in vitro and in vivo studies can be carried out based on the results of this *in silico* study.[60] Through *in silico* research, it is hoped that new antibacterial discoveries through binding mechanisms to fluoroquinolone receptors can be more quickly and easily obtained.[61] The position of compounds on amino acid residues also needs further study to better understand their relationship with antibacterial resistance. Thus efforts to obtain drugs can be more efficient through initial studies *in silico*.

CONCLUSION

All compounds can qualify for oral administration of the drug (ADMET). Curcumin and ethyl para-methoxycinnamate meet drug similarity requirements. The three-dimensional structure of the Indonesian strain of *H. pylori* has been obtained. Such structures have been used in molecular docking to obtain compounds that have potential anti-*H. pylori*. Moldock scored curcumin and hesperidin better than levofloxacin. Hesperidin does not meet the requirements for drug similarity. Moldock score ethyl para-methoxycinnamate higher than levofloxacin. From all these processes, it can be concluded that curcumin has the most potential as an anti-*H. pylori*.

ACKNOWLEDGMENTS

We thank Faculty of Medicine and Faculty of Pharmacy, Universitas Airlangga, Indonesia; the Institute of Tropical Disease (ITD), Universitas Airlangga, Indonesia; Faculty of Medicine Oita University, Yufu, Japan for providing facilities for the completion of this research.

CONFLICTS OF INTEREST

No conflict of interest

REFERENCES

1. Alexander SM, Retnakumar RJ, Chouhan D, Devi TNB, Dharmaseelan S, Devadas K, et al. Helicobacter pylori in Human Stomach: The Inconsistencies in Clinical Outcomes and the Probable Causes. Vol. 12, Frontiers in Microbiology. Frontiers Media S.A.; 2021.
2. Leja M, Grinberga-Derica I, Bilgilier C, Steininger C. Review: Epidemiology of Helicobacter pylori infection. Helicobacter. 2019 Sep 1;24(S1).
3. Zamani M, Ebrahimtabar F, Zamani V, Miller WH, Alizadeh-Navaei R, Shokri-Shirvani J, et al. Systematic review with meta-analysis: the worldwide prevalence of Helicobacter pylori infection. Aliment Pharmacol Ther [Internet]. 2018 Apr 1 [cited 2022 May 24];47(7):868–76. Available from: https://pubmed.ncbi.nlm.nih.gov/29430669/
4. Hooi JKY, Lai WY, Ng WK, Suen MMY, Underwood FE, Tanyingoh D, et al. Global Prevalence of Helicobacter pylori Infection: Systematic Review and Meta-Analysis. Gastroenterology [Internet]. 2017 Aug 1 [cited 2022 May 24];153(2):420–9. Available from: http://www.gastrojournal.org/article/S0016508517355312/fulltext
5. Miftahussurur M, Waskito LA, Fauzia KA, Mahmudah I, Doohan D, Adnyana IK, et al. Overview of helicobacter pylori infection in Indonesia: what distinguishes it from countries with high gastric cancer incidence? Gut Liver. 2021 Sep 1;15(5):653–65.
6. Syam AF, Miftahussurur M, Makmun D, Nusi IA, Zain LH, Zulkhairi, et al. Risk factors and prevalence of Helicobacter pylori in five largest islands of Indonesia: A preliminary study. PLoS One. 2015 Nov 1;10(11).
7. Yan L, Chen Y, Chen F, Tao T, Hu Z, Wang J, et al. Effect of Helicobacter pylori Eradication on Gastric Cancer Prevention: Updated Report From a Randomized Controlled Trial With 26.5 Years of Follow-up. Gastroenterology. 2022 Jul 1;163(1):154-162.e3.
8. Malfertheiner P, Megraud F, Rokkas T, Gisbert JP, Liou JM, Schulz C, et al. Management of Helicobacter pylori infection: the Maastricht VI/Florence consensus report. Gut. 2022 Sep 1;71(9):1724–62.
9. Annibale B, Esposito G, Lahner E. A current clinical overview of atrophic gastritis. Expert Rev Gastroenterol Hepatol. 2020 Feb 1;14(2):93–102.
10. Choi IJ, Kim CG, Lee JY, Kim YI, Kook MC, Park B, et al. Family History of Gastric Cancer and Helicobacter pylori Treatment. New England Journal of Medicine. 2020 Jan 30;382(5):427–36.
11. Stewart OA, Wu F, Chen Y. The role of gastric microbiota in gastric cancer. Gut Microbes. 2020 Sep 2;11(5):1220–30.
12. Wishart DS, Knox C, Guo AC, Shrivastava S, Hassanali M, Stothard P, et al. DrugBank: a comprehensive resource for *in silico* drug discovery and exploration. Nucleic Acids Res [Internet]. 2006 [cited 2022 Feb 26];34(Database issue):D668. Available from: /PMC/articles/PMC1347430/
13. Talevi A. Computer-Aided Drug Design: An Overview. Methods Mol Biol [Internet]. 2018;1762(5):1–19. Available from: http://www.ncbi.nlm.nih.gov/pubmed/29594764
14. Pinzi L, Rastelli G. Molecular docking: Shifting paradigms in drug discovery. Int J Mol Sci. 2019;20(18).
15. Aguilar-Luis MA, Palacios-Cuervo F, Espinal-Reyes F, Calderón-Rivera A, Levy-Blitchtein S, Palomares-Reyes C, et al. Highly clarithromycin-resistant Helicobacter pylori infection in asymptomatic children from a rural community of Cajamarca-Peru 11 Medical and Health Sciences 1108 Medical Microbiology. BMC Res Notes. 2018 Nov 14;11(1).
16. Botija G, García Rodríguez C, Recio Linares A, Campelo Gutiérrez C, Pérez-Fernández E, Barrio Merino A. Antibiotic resistances and eradication rates in Helicobacter pylori infection. A Pediatr (Engl Ed) [Internet]. 2021 Dec [cited 2022 Jul 22];95(6):431–7. Available from: https://pubmed.ncbi.nlm.nih.gov/34810153/

17. Miftahussurur M, Yamaoka Y. Appropriate first-line regimens to combat Helicobacter pylori antibiotic resistance: An asian perspective. Vol. 20, Molecules. MDPI AG; 2015. p. 6068–92.
18. Miftahussurur M, Shrestha PK, Subsomwong P, Sharma RP, Yamaoka Y. Emerging Helicobacter pylori levofloxacin resistance and novel genetic mutation in Nepal. BMC Microbiol. 2016 Nov 4;16(1):1–10.
19. Miftahussurur M, Syam AF, Nusi IA, Makmun D, Waskito LA, Zein LH, et al. Surveillance of Helicobacter pylori Antibiotic Susceptibility in Indonesia: Different Resistance Types among Regions and with Novel Genetic Mutations. PLoS One [Internet]. 2016 Dec 1 [cited 2022 Jan 31];11(12). Available from: https://pubmed.ncbi.nlm.nih.gov/27906990/
20. Johnston BT. Boohan M. Katzung Basic and Clinical. Vol. 34, Medical Education. 2017. 692–699 p.
21. Bush NG, Diez-Santos I, Abbott LR, Maxwell A. Quinolones: Mechanism, Lethality and Their Contributions to Antibiotic Resistance. Molecules [Internet]. 2020 Dec 1 [cited 2022 May 22];25(23). Available from: /PMC/articles/PMC7730664/
22. Gollapalli P, Tamizh Selvan G, Santoshkumar HS, Ballamoole KK. Functional insights of antibiotic resistance mechanism in Helicobacter pylori: Driven by gene interaction network and centrality-based nodes essentiality analysis. Microb Pathog. 2022 Oct;171:105737.
23. Martínez-Júlvez M, Rojas AL, Olekhnovich I, Angarica VE, Hoffman PS, Sancho J. Structure of RdxA: an oxygen insensitive nitroreductase essential for metronidazole activation in Helicobacter pylori. FEBS J [Internet]. 2012 Dec [cited 2022 Sep 6];279(23):4306. Available from: /PMC/articles/PMC3504637/
24. Vijayakumar K, Muhilvannan S, Arun Vignesh M. Hesperidin inhibits biofilm formation, virulence, and staphyloxanthin synthesis in methicillin-resistant Staphylococcus aureus by targeting SarA and CrtM: an in vitro and *in silico* approach. World J Microbiol Biotechnol [Internet]. 2022 Mar 1 [cited 2022 Apr 23];38(3):1–12. Available from: https://link.springer.com/article/10.1007/s11274-022-03232-5
25. Zheng D, Huang C, Huang H, Zhao Y, Khan MRU, Zhao H, et al. Antibacterial Mechanism of Curcumin: A Review. Chem Biodivers [Internet]. 2020 Aug 1 [cited 2022 Apr 13];17(8). Available from: https://pubmed.ncbi.nlm.nih.gov/32533635/
26. Barua N, Buragohain AK. Therapeutic Potential of Curcumin as an Antimycobacterial Agent. Biomolecules 2021, Vol 11, Page 1278 [Internet]. 2021 Aug 26 [cited 2022 Apr 12];11(9):1278. Available from: https://www.mdpi.com/2218-273X/11/9/1278/htm
27. Zorofchian Moghadamtousi S, Abdul Kadir H, Hassandarvish P, Tajik H, Abubakar S, Zandi K. A Review on Antibacterial, Antiviral, and Antifungal Activity of Curcumin. Biomed Res Int [Internet]. 2014 [cited 2022 Apr 13];2014. Available from: /PMC/articles/PMC4022204/
28. Olszewska MA, Gedas A, Simões M. The effects of eugenol, trans-cinnamaldehyde, citronellol, and terpineol on Escherichia coli biofilm control as assessed by culture-dependent and -independent methods. Molecules. 2020 Jun 1;25(11).
29. Millezi AF, Costa KAD, Oliveira JM, Lopes SP, Pereira MO, Piccoli RH. Antibacterial and anti-biofilm activity of cinnamon essential oil and eugenol. Ciencia Rural. 2019;49(1).
30. Ali SM, Khan AA, Ahmed I, Musaddiq M, Ahmed KS, Polasa H, et al. Antimicrobial activities of Eugenol and Cinnamaldehyde against the human gastric pathogen Helicobacter pylori. Ann Clin Microbiol Antimicrob [Internet]. 2005 Dec 21 [cited 2022 Mar 27];4. Available from: https://pubmed.ncbi.nlm.nih.gov/16371157/
31. Kataria R, Khatkar A. Molecular docking, synthesis, kinetics study, structure-activity relationship, and ADMET analysis of morin analogous as Helicobacter pylori urease inhibitors. BMC Chem [Internet]. 2019 Apr 1 [cited 2022 Apr 24];13(3):1–17. Available from: https://bmcchem.biomedcentral.com/articles/10.1186/s13065-019-0562-2
32. Fong P, Hao CH, Io CC, Sin PI, Meng LR. *In silico* and in vitro anti-Helicobacter pylori effects of combinations of phytochemicals and antibiotics. Molecules [Internet]. 2019;24(19). Available from: www.mdpi.com/journal/molecules
33. Pasala C, Katari SK, Nalamolu RM, Bitla AR, Amineni U. *In silico* probing exercises, bioactive-conformational and dynamic simulations strategies for designing and promoting selective therapeutics against Helicobacter pylori strains. J Mol Graph Model. 2019 Nov 1;92:167–79.
34. Kim S. Exploring Chemical Information in PubChem. Curr Protoc [Internet]. 2021 Aug 1 [cited 2022 Feb 27];1(8). Available from: /PMC/articles/PMC8363119/
35. Bienert S, Waterhouse A, De Beer TAP, Tauriello G, Studer G, Bordoli L, et al. The SWISS-MODEL Repository—new features and functionality. Nucleic Acids Res [Internet]. 2017 Jan 1 [cited 2022 Feb 27];45(Database issue): D313. Available from: /PMC/articles/PMC5210589/
36. Waterhouse A, Bertoni M, Bienert S, Studer G, Tauriello G, Gumienny R, et al. SWISS-MODEL: homology modeling of protein structures and complexes. Nucleic Acids Res [Internet]. 2018 Jul 7 [cited 2022 Sep 16];46(Web Server issue):W296. Available from: /PMC/articles/PMC6030848/
37. Daina A, Michielin O, Zoete V. SwissADME: a free web tool to evaluate pharmacokinetics, drug-likeness and medicinal chemistry friendliness of small molecules OPEN. Nature Publishing Group [Internet]. 2017; Available from: http://www.swissadme.ch
38. Pires DE V, Blundell TL, Ascher DB, 1ga UK. pkCSM: Predicting Small-Molecule Pharmacokinetic and Toxicity Properties Using Graph-Based Signatures. 2015 [cited 2022 Jun 23]; Available from: http://structure.bioc.cam.ac.uk/
39. Thomsen R, Christensen MH. MolDock: a new technique for high-accuracy molecular docking. J Med Chem [Internet]. 2006 Jun 1 [cited 2023 Nov 12];49(11):3315–21. Available from: https://pubmed.ncbi.nlm.nih.gov/16722650/
40. Biovia Discovery Studio Overview.
41. Bitencourt-Ferreira G, de Azevedo WF. Molegro virtual docker for docking. Methods in Molecular Biology [Internet]. 2019 [cited 2023 Apr 8];2053:149–67. Available from: https://link.springer.com/protocol/10.1007/978-1-4939-9752-7_10
42. Merck molecular force field. V. Extension of MMFF94 using experimental data, additional computational data, and empirical rules - Halgren - 1996 - Journal of Computational Chemistry - Wiley Online Library [Internet]. [cited 2023 Nov 12]. Available from: https://onlinelibrary.wiley.com/doi/10.1002/%28SICI%291096-987X%28199604%2917%3A5/6%3C616%3A%3AAID-JCC5%3E3.0.CO%3B2-X
43. Sulistyowaty MI, Widyowati R, Putra GS, Budiati T, Matsunami K. Synthesis, ADMET predictions, molecular docking studies, and in-vitro anticancer activity of some benzoxazines against A549 human lung cancer cells. J Basic Clin Physiol Pharmacol. 2021 Jul 1;32(4):385–92.
44. Stank A, Kokh DB, Fuller JC, Wade RC. Protein Binding Pocket Dynamics. Acc Chem Res [Internet]. 2016 May 17 [cited 2022 Sep 16];49(5):809–15. Available from: https://pubs.acs.org/doi/full/10.1021/acs.accounts.5b00516
45. He Y, Cheng P, Wang W, Yan S, Tang Q, Liu D, et al. Rapid investigation and screening of bioactive components in simo decoction via LC-Q-TOF-MS and UF-HPLC-MD methods. Molecules. 2018 Jan 1;23(7):1792.
46. Nandeesh R, Vijayakumar S, Munnolli A, Alreddy A, Veerapur VP, Chandramohan V, et al. Bioactive phenolic fraction of Citrus maxima abate lipopolysaccharide-induced sickness behavior and anorexia in mice: In-silico molecular docking and dynamic studies of biomarkers against NF-κB. Biomedicine and Pharmacotherapy. 2018 Dec 1;108:1535–45.

47. Zeenat L, Prajapati S, Sangeet S, Khan A, Pandey KM. In-silico Screening of Potential Phytochemicals against Extracellular Adherence (Eap) Protein of Staphylococcus aureus from Indian Medicinal Plants. Res J Pharm Technol. 2023 Oct 1;16(10):4691–7.

48. Sharma HK, Gupta P, Nagpal D, Mukherjee M, Parmar VS, Lather V. Virtual screening and antimicrobial evaluation for identification of natural compounds as the prospective inhibitors of antibacterial drug resistance targets in Staphylococcus aureus. Fitoterapia. 2023 Jul 1;168:105554.

49. Pantsar T, Poso A. Binding affinity via docking: Fact and fiction. Vol. 23, Molecules. MDPI AG; 2018. p. 1DUMMY.

50. Rampogu S, Balasubramaniyam T, Lee JH. Curcumin Chalcone Derivatives Database (CCDD): a Python framework for natural compound derivatives database. PeerJ. 2023 Jan 1;11:e15885.

51. Samreen, Qais FA, Ahmad I. *In silico* screening and in vitro validation of phytocompounds as multidrug efflux pump inhibitor against E. coli. J Biomol Struct Dyn. 2023 Jan 1;41(6):2189–201.

52. Lipinski CA, Lombardo F, Dominy BW, Feeney PJ. Experimental and computational approaches to estimate solubility and permeability in drug discovery and development settings. Adv Drug Deliv Rev. 2001 Mar 1;46(1–3):3–26.

53. Lipinski CA. Rule of five in 2015 and beyond Target and ligand structural limitations, ligand chemistry structure, and drug discovery project decisions. Vol. 101, Advanced Drug Delivery Reviews. Elsevier B.V.; 2016. p. 34–41.

54. Khairullah AR, Solikhah TI, Ansori ANM, Hanisia RH, Puspitarani GA, Fadholly A, et al. Medicinal importance of kaempferia galanga l. (Zingiberaceae): A comprehensive review. Vol. 10, Journal of HerbMed Pharmacology; 2021. p. 281–8.

55. Prasetyanti IK, Sukardiman, Suharjono. ADMET Prediction and *In silico* Analysis of Mangostin Derivatives and Sinensetin on Maltase-Glucoamylase Target for Searching Anti-Diabetes Drug Candidates. Pharmacognosy Journal. 2021 Jul 1;13(4):883–9.

56. Phucharoenrak P, Muangnoi C, Trachootham D. A Green Extraction Method to Achieve the Highest Yield of Limonin and Hesperidin from Lime Peel Powder (Citrus aurantifolia). Molecules [Internet]. 2022 Feb 1 [cited 2022 Apr 20];27(3). Available from: /PMC/articles/PMC8840237/

57. Verma AK, Ahmed SF, Hossain MS, Bhojiya AA, Mathur A, Upadhyay SK, et al. Molecular docking and simulation studies of flavonoid compounds against PBP-2a of methicillin-resistant Staphylococcus aureus. J Biomol Struct Dyn. 2022 Jan 1;40(21):10561–77.

58. Zelelew D, Endale M, Melaku Y, Geremew T, Eswaramoorthy R, Tufa LT, et al. Ultrasonic-Assisted Synthesis of Heterocyclic Curcumin Analogs as Antidiabetic, Antibacterial, and Antioxidant Agents Combined with in vitro and silico Studies. Advances and Applications in Bioinformatics and Chemistry. 2023;16:61–91.

59. Varadi M, Anyango S, Deshpande M, Nair S, Natassia C, Yordanova G, et al. AlphaFold Protein Structure Database: massively expanding the structural coverage of protein-sequence space with high-accuracy models. Nucleic Acids Res [Internet]. 2022 Jan 7 [cited 2022 Sep 7];50(D1):D439–44. Available from: https://academic.oup.com/nar/article/50/D1/D439/6430488

60. Sathianarayanan S, Ammanath AV, Biswas R, B A, Sukumaran S, Venkidasamy B. A new approach against Helicobacter pylori using plants and its constituents: A review study. Microb Pathog. 2022 Jul 1;168.

61. Abdel-Aziz SA, Cirnski K, Herrmann J, Abdel-Aal MAA, Youssif BGM, Salem OIA. Novel fluoroquinolone hybrids as dual DNA gyrase and urease inhibitors with potential antibacterial activity: Design, synthesis, and biological evaluation. J Mol Struct. 2022 Sep;134049.

62. Herdiansyah MA, Ansori ANM, Kharisma VD, et al. *In silico* study of cladosporol and its acyl derivatives as anti-breast cancer againts alpha-estrogen receptor. Biosaintifika. 2024;16(1): 142-154.

63. Zainul R, Kharisma VD, Ciuputri P, et al. Antiretroviral activity from elderberry (Sambucus nigra L.) flowers against HIV-2 infection via reverse transcriptase inhibition: a viroinformatics study. Healthcare in Low-resource Settings. 2024;1(2024): 1-12.

64. Krihariyani D, Haryanto E, Sasongkowati R. In Silico Analysis of Antiviral Activity and Pharmacokinetic Prediction of Brazilein Sappan Wood (Caesalpinia sappan L.) Against SARS-CoV-2 Spike Glycoproteins. Indonesian Journal of Medical Laboratory Science and Technology. 2021; 3(1): 26–37.

GRAPHICAL ABSTRACT

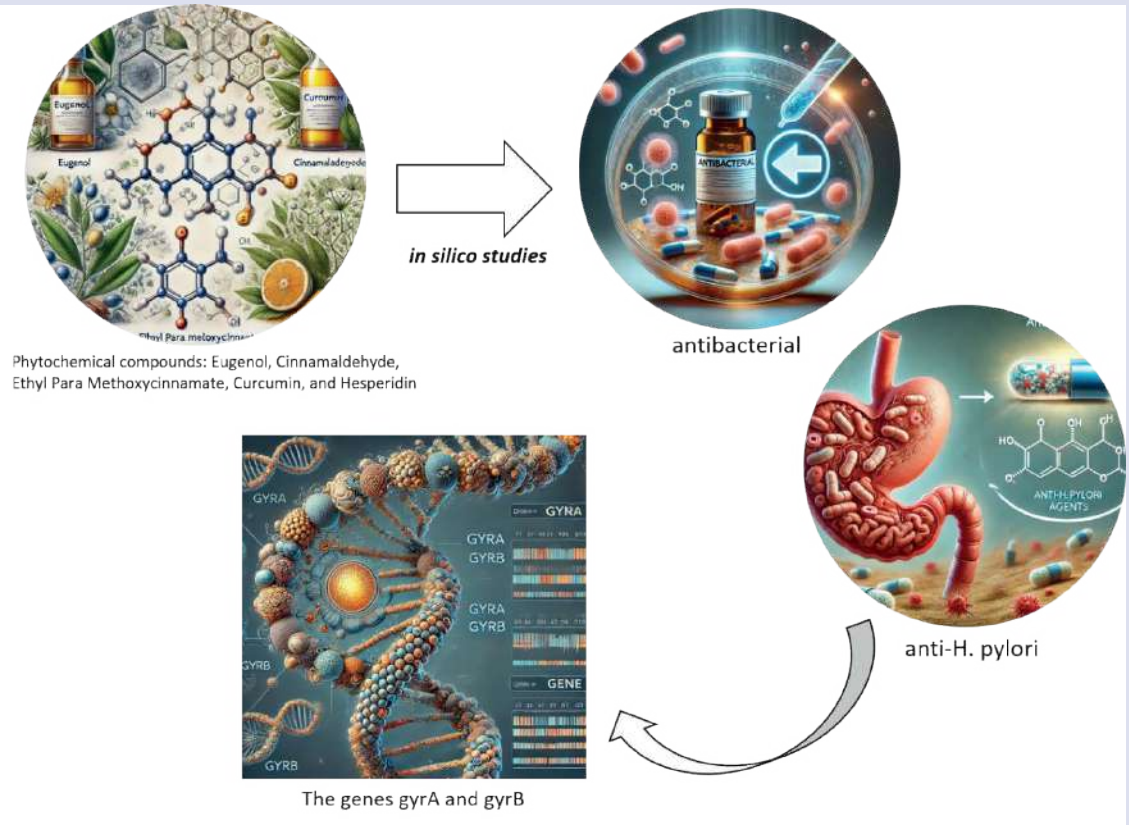

ABOUT AUTHORS

Musa Ghufron
Musa Ghufron is a doctoral program student at Universitas Airlangga Surabaya, Indonesia. His research projects are related to bioinformatics and computational medicine.

Rahadian Zainul
Rahadian Zainul is a Professor in Physical Chemistry and a Researcher in CAMPBIOTICS, Universitas Negeri Padang, Indonesia. His research projects are related to bioinformatics and advanced material and also in computational chemistry. He is also as Felow Researcher at INTI International University, Malaysia.

Cite this article: Ghufron M, Sukardiman, Zainul R, Miftahussurur M, Ansori ANM, Herdiansyah MA. In Silico Study of Eugenol, Cinnamaldehyde, Ethyl Para Methoxycinnamate, Curcumin, and Hesperidin as Antibacterials Against Levofloxacine-Resistant Indonesian H. pylori Strains. Pharmacogn J. 2024;16(4): 816-830.